

## SIMULATING TRIGGERING AND EVOLUTION OF DEBRIS-FLOWS WITH SPH

GIACOMO VICCIONE<sup>(\*)</sup> & VITTORIO BOVOLIN<sup>(\*)</sup>

<sup>(\*)</sup>University of Salerno, Department of Civil Engineering - Via Ponte Don Melillo - 84084 - Fisciano (Italy)  
Email: gviccion@unisa.it

### ABSTRACT

Recently, debris-flow kinds of phenomena have been reproduced by means of Lagrangian methods, such as Distinct Element Method (DEM) or Lagrangian Finite Element Method (LFEM). Among the others, meshless, Lagrangian numerical method, known as Smoothed Particle Hydrodynamics (SPH), is here applied to simulate debris-flow initiation and propagation over the slope of a mountain located in the city of Nocera Inferiore (Southern Italy). Debris-flows have been simulated since long time for hazard mitigation assessment or deposit evaluation via Eulerian-based methods. Since they may feature mesh distortion as the computational domain evolves, heavy grid refinement algorithms are sometimes necessary, especially for those problems characterized by large deformations. SPH overcomes such difficulties since no mesh is needed over the physical domain. Spatial discretization is indeed carried out with a collection of particles without connectivity bonds among them. While boundary particles are fixed over time, computing particles are free to move in response of external and internal forces such as gravity and pressure.

More in detail, computing particles are all initially frozen. Once a particle located in the upper region of the slope is set free, the others close to it move if a pressure threshold  $p_{lim}$  is reached. Other particles are subsequently triggered where the mentioned condition occur, as a domino effect. Runout velocity is controlled by handling the shear stress  $\tau_{bed}$  with the fixed bed.

Results show how different are the conditions of motion, by varying the location of the triggering area, the pressure threshold  $p_{lim}$  and the shear stress  $\tau_{bed}$ . In order to measure the capability of SPH into simulating such events, some comparisons are made with corresponding Flo 2D results.

**KEY WORDS:** SPH, debris-flow initiation, debris-flow propagation

### INTRODUCTION

Debris flow usually take place on steep slopes after heavy or long rainfall events, mobilizing loose material, such as soil, vegetation, debris ranging from clays to boulders. They may represent a threat for people living nearby such areas and for buildings, i.e. bridges, facilities, etc. Therefore, understanding the movement mechanism is of considerable interest, particularly in the evaluation of potential mitigation policies (TAKAHASHI, 1991; IVERSON, 1997). In addition to precipitations, landslide mechanics depend on several factors, such as type of weather, morphology, geology, land use and plant growth. In this work, we only investigate about the ability of simulating debris-flow initiation and subsequent movement with the Smoothed Particle Hydrodynamics (SPH) technique. Triggering is here settled randomly, making free to move a particle located in the upper part of the slope being considered. The others are all initially frozen. Motion of remaining particles is related to the achievement of a pressure threshold  $p_{lim}$  (Fig. 1). The resulting process is like a domino effect or a cascading failure.

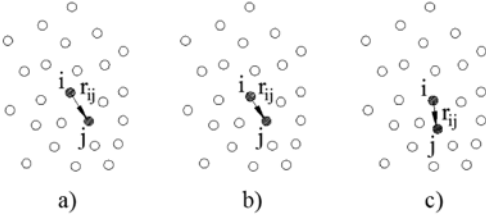


Fig. 1 - Neighbour particle destabilization. a) Particle “i” is approaching the neighbour particle “j”. b) Despite the relative distance “ $r_{ij}$ ” is decreased, particle “j” is still fixed because  $p_{ij} < p_{lim}$ . c) Particle “j” is set free to move because the interstitial pressure “ $p_{ij}$ ” has reached the threshold value “ $p_{lim}$ ”

Computing particles are initially set with a pressure being equal to the atmospheric value. The relative spatial allocation is obtained with a specific mesh generator, which guarantees a distribution of points forming triangles approximately equilaterals. While some particles are moving, they may approach others initially still, to the point for which the relative distance yields a pressure greater than a threshold value. Once reached such point, those neighbouring particles, previously fixed, are then set free to move.

## NUMERICAL APPROACH

Debris-flow initiation and subsequent evolution is here simulated with the Smoothed Particle Hydrodynamics technique. Introduced three decades ago for astrophysical applications (GINGOLD & MONAGHAN, 1977; LUCY, 1977), it has been subsequently applied in many other and different research areas such as multi-phase flows (MONAGHAN & KOCHARYAN, 1995), flows through porous media (MORRIS *et alii*, 1999; ZHU *et alii*, 1999), high explosive detonation and explosion (SWEGLE & ATTAWAY, 1995; LIU *et alii*, 2000), hyper velocity impact and penetration (ZUKAS, 1990; RANDES & LIBERSKY, 1996).

Such as a meshless, Lagrangian, particle method, the SPH method presents some special advantages over the traditional grid-based methods. Among the others, the most appealing feature is the adaptive nature which means that is not affected by arbitrariness of particle distribution. Indeed, there is no need to prescribe the connectivity between the moving particles. With such technique, computing particles carry physical properties such as velocity or density. Advection is exactly computed without numerical errors. More consideration has been subsequently devoted to SPH as good choice for geomechanical problems.

With this technique, non-linear partial differential equations of Navier-Stokes (BATCHELOR, 1974) are adapted as follows:

$$\rho \frac{D\mathbf{v}}{Dt} = -\nabla p + \boldsymbol{\tau}_{int} + \boldsymbol{\tau}_{bed} + \underline{\mathbf{f}} \quad (1.a)$$

$$\frac{D\rho}{Dt} + \rho \nabla \cdot \underline{\mathbf{v}} = 0 \quad (1.b)$$

where  $\rho$  is the density,  $\underline{\mathbf{v}}$  the velocity,  $p$  the pressure,  $\boldsymbol{\tau}_{int}$  the internal viscous shear stress,  $\boldsymbol{\tau}_{bed}$  the internal viscous shear stress,  $\underline{\mathbf{f}}$  the external forces per unit of volume.

The above equations of conservation are then discretized on particle position (LIU & LIU, 2003), yielding the following new set of equations:

$$\frac{d\underline{\mathbf{v}}_i}{dt} = -\sum_{j=1}^N m_j \left( \frac{p_j}{\rho_j^2} + \frac{p_i}{\rho_i^2} + \Pi_{ij} \right) \nabla_i W_{ij} + \underline{\mathbf{g}} \quad (2.a)$$

$$\frac{dp_i}{dt} = \sum_{j=1}^N m_j (\underline{\mathbf{v}}_i - \underline{\mathbf{v}}_j) \cdot \nabla_i W_{ij} \quad (2.b)$$

in which viscous terms are modelled with the following artificial viscosity model:

$$\Pi_{ij} = \frac{-\alpha_k c_{ij} \mu_{ij} + \beta \mu_{ij}^2}{\rho_{ij}} \quad (3)$$

where

$$\mu_{ij} = \frac{s \underline{\mathbf{v}}_{ij} \cdot \underline{\mathbf{x}}_{ij}}{x_{ij} + \eta^2} \quad (4)$$

The notation  $\bar{a}_{ij} = (a_i + a_j) / 2$ ,  $b_{ij} = b_i - b_j$  has been used above. Sums appearing in Equations 2 refer to the neighbouring particles within a short range “ $r_c$ ” (Figure 2) respect to the particle “i”. “W” (Figure 3) is the weighing or kernel function (MONAGHAN & LATTANZIO, 1985), whose expression is given by the following:

$$W(q, h) = A_n (n_d) \cdot \begin{cases} \frac{2}{3} - q^2 + \frac{1}{2} q^3 & 0 \leq q < 1 \\ \frac{1}{6} (2 - q)^3 & 1 \leq q < 2 \\ 0 & q \geq 2 \end{cases} \quad (5)$$

in which  $q = |x_i - x_j| / 2 \cdot r_c$  is the relative dimensionless distance between “i” and “j” particles,  $A = 10/7 \cdot \pi$  or  $A = 1/\pi$  respectively for 2-dimensional ( $n_d = 2$ ) or 3-dimensional ( $n_d = 3$ ) problems.

“ $\alpha_k$ ” is the linear viscosity coefficient (MONAGHAN, 1994) taken to be fixed ( $\alpha_k = \alpha_{int} = 0,1$ ) when particle “i” interacts with another computing particle “j”, or variable ( $\alpha_k = \alpha_{bed}$ ) when particle “j” is a boundary one; “ $\beta$ ” is always set to be 0, i.e. the nonlinear term in  $\Pi_{ij}$  is not taken into account.

The term “c” represents the speed of sound whose order of magnitude is ten times greater than the maximum estimate of the velocity field, “v” and “x” repre-

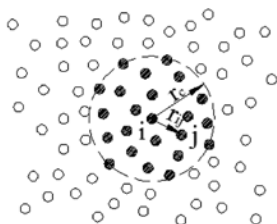


Fig. 2 - Short range interactions. Properties of particle “i” are computed on the basis of those particles within a cut-off distance “rc” (bold marked). Outer particles give no contribution

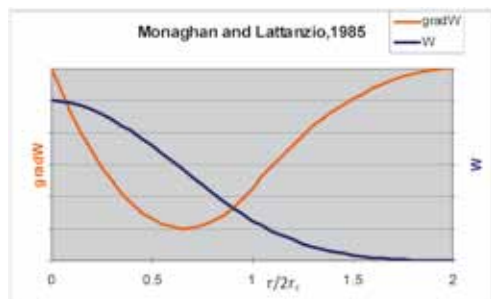


Fig. 3 - Smoothing kernel adopted with its gradient

sent the velocity and position respectively,  $\eta = 0.05 \cdot r_c$  is employed to prevent numerical divergences when two particles are colliding.

It should be noted that the artificial viscosity is both function of the relative position and velocity, that is  $\Pi_{ij} = \Pi_{ij}(x_{ij}, v_{ij})$ .

Since no connectivity is established among the particles, Neighbourhood identification is carried out by means of a special search algorithm (VICCIONE *et alii*, 2008).

The correction XSPH (MONAGHAN, 1994) on the time derivative of particle position

$$\frac{Dx_i}{Dt} = \underline{v}_i \tag{5.bis}$$

has been adopted, by adding the following quantity to the right hand side of Equation 5:

$$\Delta v_i = 0.5 \sum_{j=1}^N \frac{m_j (v_j - v_i)}{\rho_{ij}} W_{ij} \tag{6}$$

doing so, each particle is locally constrained to move with a velocity depending on the average value of its neighbourhood. This is useful in the case of high velocity or impact problems, because it avoids unphysical flow separation.

Closure is assured by adding an equation of state, describing the relationship between density and pressure. As a matter of facts, for near incompressible media, the real equation of state determines time steps

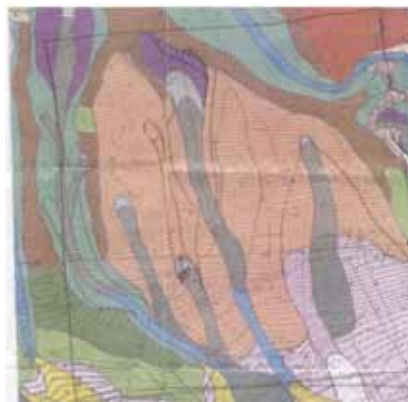


Fig. 4 - Map location of the area, object of the investigation

extremely small. In the present work a stiff equation of state is assumed (BATCHELOR, 1974):

$$p_i = B \left[ \left( \frac{\rho_i}{\rho_0} \right)^\gamma - 1 \right] \tag{7}$$

with  $\gamma = 7$ ,  $\rho_0 = 2600\text{kg/m}^3$  is the reference density of the superficial soil within the area of investigation and “B” is given by:

$$B = \frac{c_0^2 \rho_0}{\gamma} \tag{8}$$

in which the reference speed of sound “c<sub>0</sub>” is chosen considering a small Mach number  $M_{ac} = 0.1 \div 0.01$  (MONAGHAN, 1994).

### DEBRIS FLOW SIMULATION

The SPH based code has been used for a preliminary study of debris-flow triggering and propagation over a slope located in the area of Nocera Inferiore (Italy). The area, object of study, is shown in the next Figure 4.

The available domain has been discretized with GiD® software. (GID Reference manual, 2009) The resulting grid mesh is well performed, with a reference distance being  $d_0 = 2.5$  m and particles forming triangles as equilateral as possible. A single layer of moving particles has been laid on the upper part of the slope (blue region in the Figure 5). The total number of moving and boundary particles are respectively  $N_f = 5000$  and  $N_{bound} = 11000$ .

All moving particles are initially fixed. Basically the motion is made by unfreezing a particle located in the upper part of the slope. Such region is schematically shown in the above figure with red circles. The subsequent mobilization along the slope is subordinated by the achievement of a particle pressure greater than a lim-

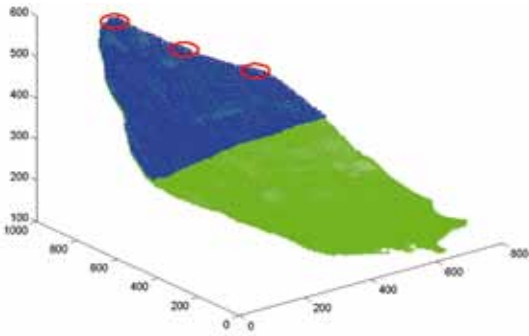


Fig. 5 - Spatial discretization of the study area. Red circles represent the region where a local triggering is imposed

it value " $p_{lim}$ ". Propagation velocity is handled by varying the bed shear stress whose expression is assumed to be equal to the artificial viscosity (Eq. 3) introduced by (MONAGHAN, 1994). Different values of the linear coefficient  $\alpha_{bed}$ , are assumed. The following Table 1 shows the simulations carried out, with specification of the triggering particles and of the parameters above introduced.

The next Figures 6 to 16 illustrate three instants for each SPH based simulation, with the indication of the area been mobilized. Following a previous study (VICCIONE & BOVOLIN, 2010), the authors have also carried out some simulation with Flo-2D (FLO-2D user manual, 2009) as shown from Figure 17 to Figure 22, willing to perform a comparison for simulation times  $t = 50$  sec and  $t = 100$  sec, with the corresponding SPH results shown in Figure 6 (Simul. N. 1), Figure 11 (Simul. N. 6) and Figure 14 (Simul. N. 9), showing a good agreement in terms of both mobilized volumes and front propagation.

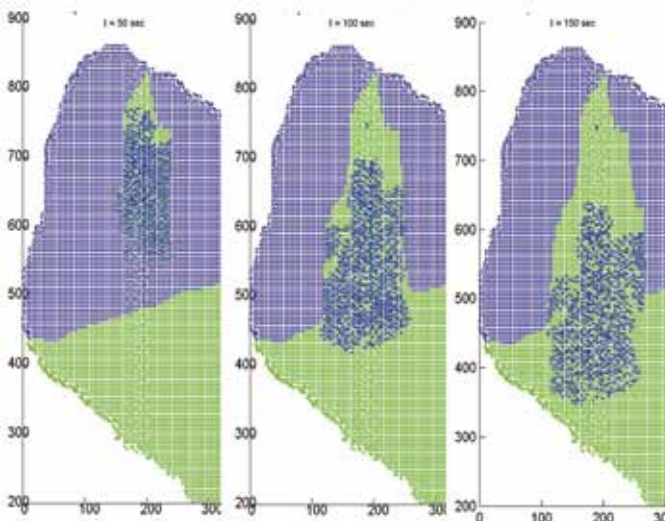


Fig. 6 - Simul. N.1. Particle triggered: PT1, limit pressure  $p_{lim} = 300 \text{ kgf/cm}^2$ , viscosity coefficient  $\alpha_{bed} = 0.1$

Simul.	Triggering coords.	ID of the trig. particle	Plim [ $\text{kgf/cm}^2$ ]	$\alpha_{bed}$
1	199.50; 821.97; 435.43	PT1	300	0.1
2	199.50; 821.97; 435.43	PT1	200	0.1
3	199.50; 821.97; 435.43	PT1	100	0.1
4	308.25; 758.05; 377.01	PT2	300	0.1
5	308.25; 758.05; 377.01	PT2	200	0.1
6	308.25; 758.05; 377.01	PT2	100	0.1
7	422.11; 688.68; 325.71	PT3	300	0.1
8	422.11; 688.68; 325.71	PT3	200	0.1
9	422.11; 688.68; 325.71	PT3	100	0.1
10	422.11; 688.68; 325.71	PT3	200	1
11	422.11; 688.68; 325.71	PT3	200	10

Tab. 1 - List of simulations been carried out

## CONCLUSIONS

As can be seen from the above Figures, varying the location of the triggering area, the limit pressure  $p_{lim}$  and the shear stress  $\tau_{bed}$ , the condition of motion are quite different. More specifically, the area been mobilized become larger when decreasing the isotropic pressure  $p_{lim}$ . At the same time, by increasing the shear stress with the bed, the front wave propagates slower, according to the common experience. A comparative analysis of SPH results with Flo-2D commercial code has been carried out, obtaining a good agreement in terms of both mobilized volumes and front propagation.

## ACKNOWLEDGEMENTS

The authors wish to thank for the support coming from the University Consortium for Research on Major Hazards (CUGRI), with special regard to the director, Prof. Eugenio Pugliese Carratelli. The authors are also in debt with Ing. Nicola Immediata from the University of Salerno, for his precious contribution and for helpful comments concerning this work.

Fig. 7 - Simul. N.2. Particle triggered: PT1, limit pressure  $p_{lim} = 200 \text{ kgf/cm}^2$ , viscosity coefficient  $\alpha_{bed} = 0.1$

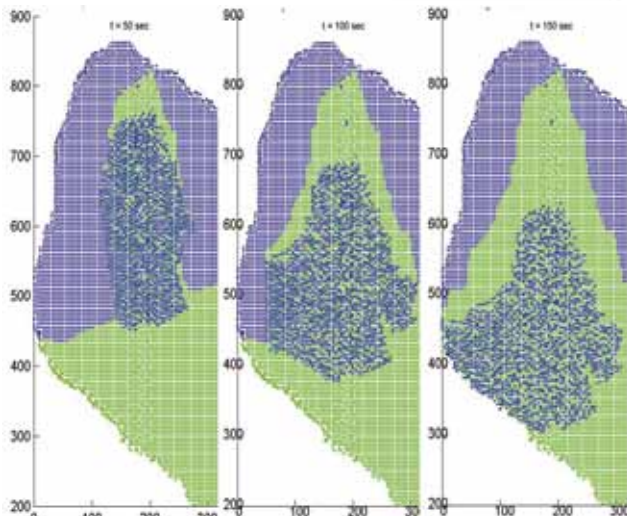
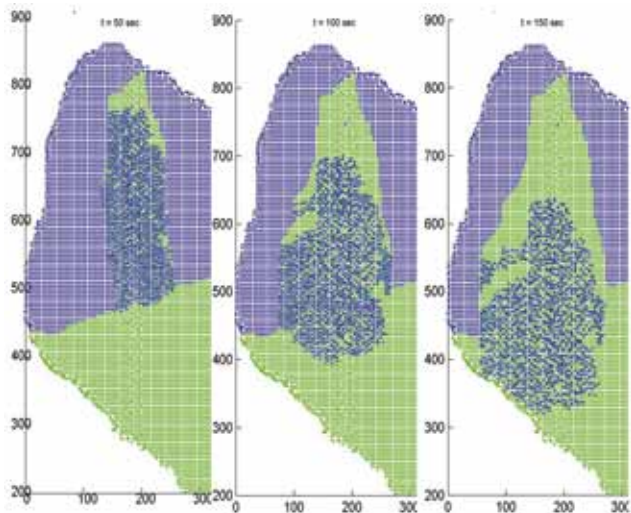
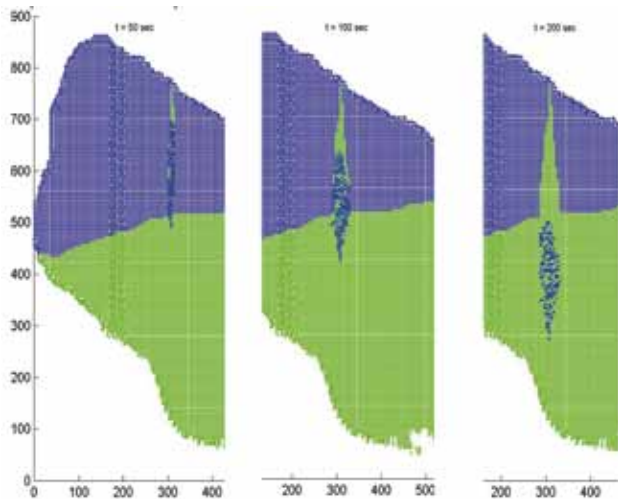


Fig. 8 - Simul. N.3. Particle triggered: PT1, limit pressure  $p_{lim} = 100 \text{ kgf/cm}^2$ , viscosity coefficient  $\alpha_{bed} = 0.1$

Fig. 9 - Simul. N.4. Particle triggered: PT2, limit pressure  $p_{lim} = 300 \text{ kgf/cm}^2$ , viscosity coefficient  $\alpha_{bed} = 0.1$



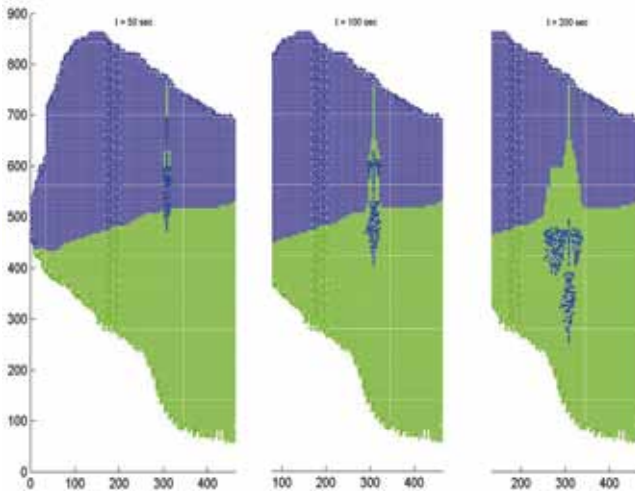


Fig. 10 - Simul. N.5. Particle triggered: PT2, limit pressure  $p_{lim} = 200 \text{ kgf/cm}^2$ , viscosity coefficient  $\alpha_{bed} = 0.1$

Fig. 11 - Simul. N.6. Particle triggered: PT2, limit pressure  $p_{lim} = 100 \text{ kgf/cm}^2$ , viscosity coefficient  $\alpha_{bed} = 0.1$

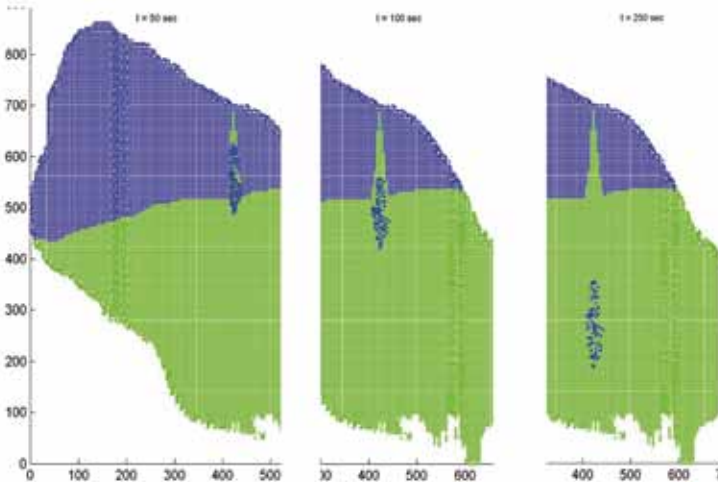
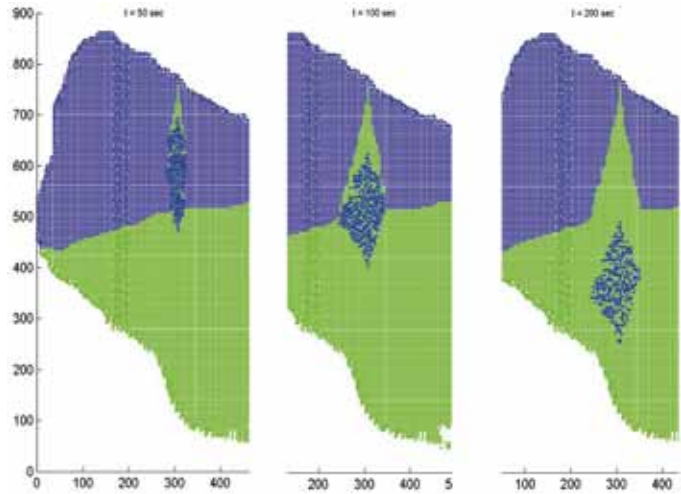


Fig. 12 - Simul. N.7. Particle triggered: PT3, limit pressure  $p_{lim} = 300 \text{ kgf/cm}^2$ , viscosity coefficient  $\alpha_{bed} = 0.1$

Fig. 13 - Simul. N.8. Particle triggered: PT3, limit pressure  $p_{lim} = 200 \text{ kgf/cm}^2$ , viscosity coefficient  $\alpha_{bed} = 0.1$

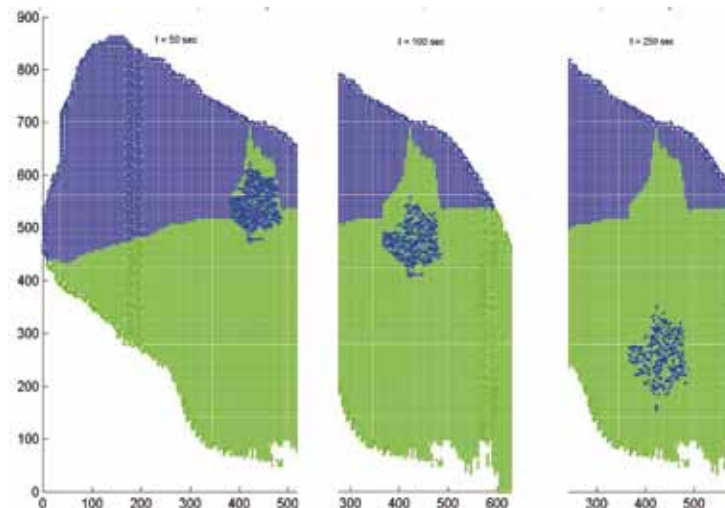
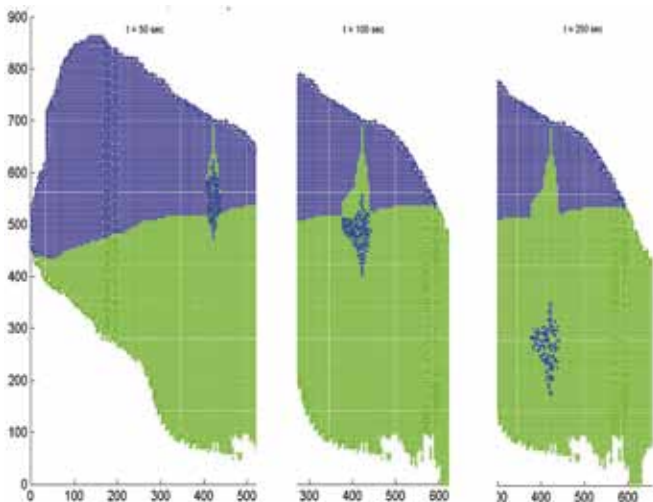
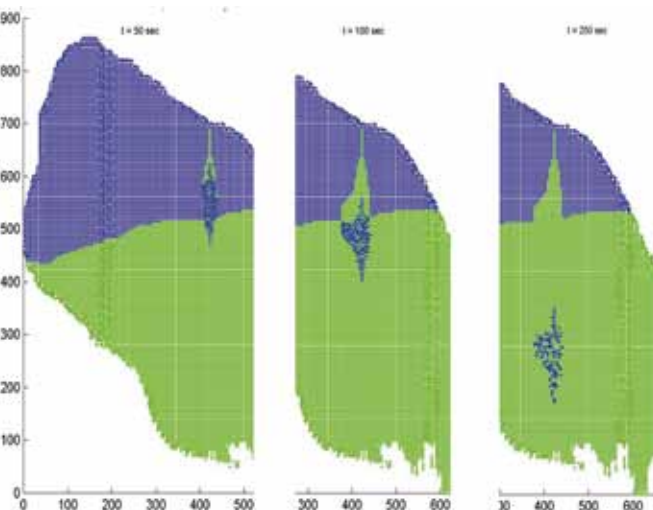


Fig. 14 - Simul. N.9. Particle triggered: PT3, limit pressure  $p_{lim} = 100 \text{ kgf/cm}^2$ , viscosity coefficient  $\alpha_{bed} = 0.1$

Fig. 15 - Simul. N.10. Particle triggered: PT3, limit pressure  $p_{lim} = 200 \text{ kgf/cm}^2$ , viscosity coefficient  $\alpha_{bed} = 1$



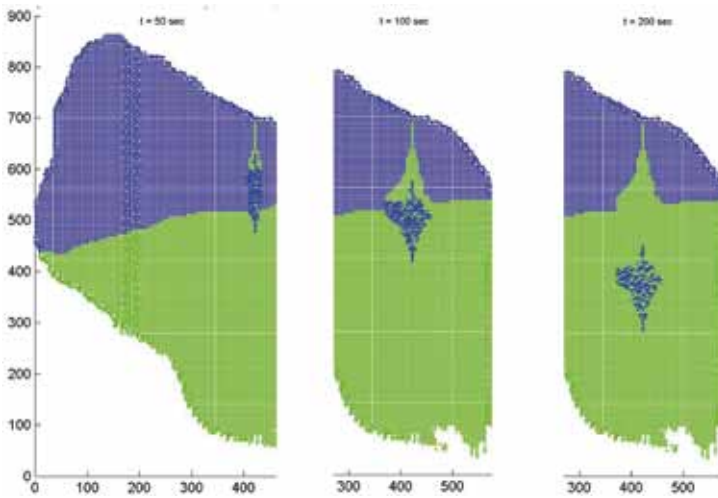


Fig. 16 - Simul. N.10. Particle triggered: PT3, limit pressure  $p_{lim} = 200 \text{ kgf/cm}^2$ , viscosity coefficient  $\alpha_{bed} = 10$

Fig. 17 - Comparison between Simul. N.1. and Flo-2D results for  $t = 50 \text{ secs}$

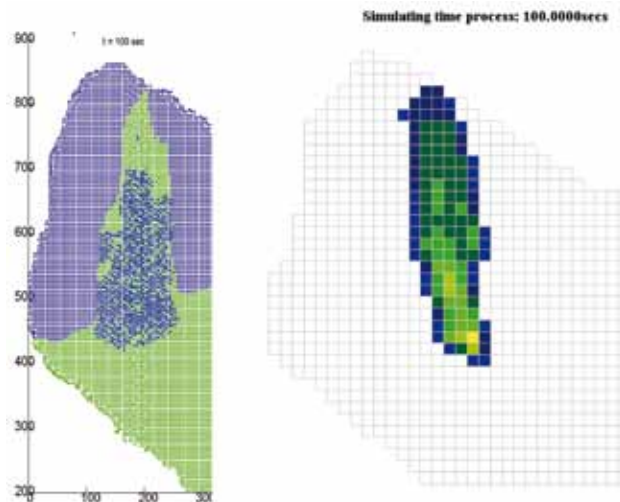
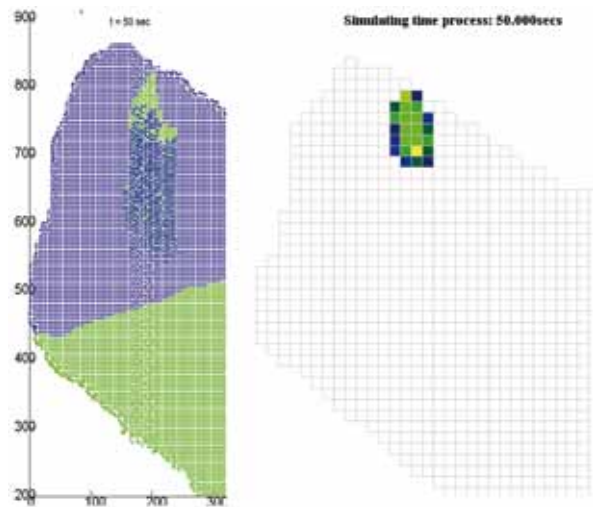


Fig. 18 - Comparison between Simul. N.1. and Flo-2D results for  $t = 100 \text{ secs}$



Fig. 19 - Comparison between Simul. N.6. and Flo-2D results for  $t = 50$  secs

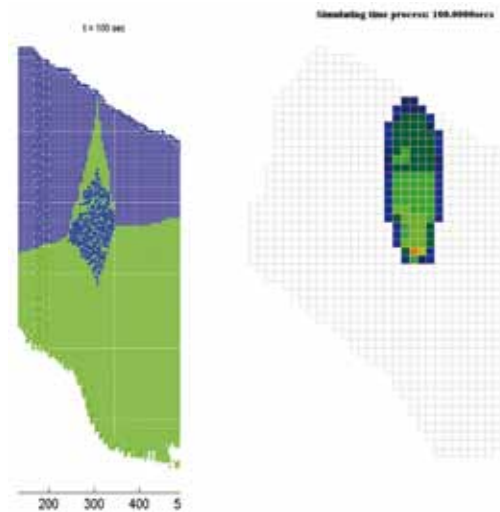
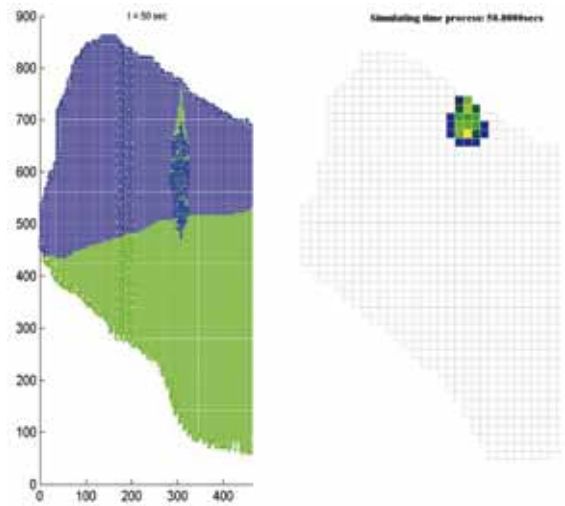
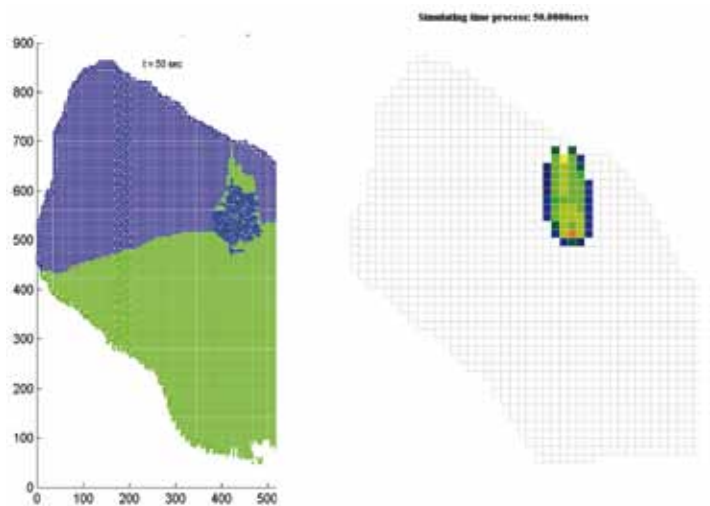


Fig. 20 - Comparison between Simul. N.6. and Flo-2D results for  $t = 100$  secs

Fig. 21 - Comparison between Simul. N.9. and Flo-2D results for  $t = 50$  secs



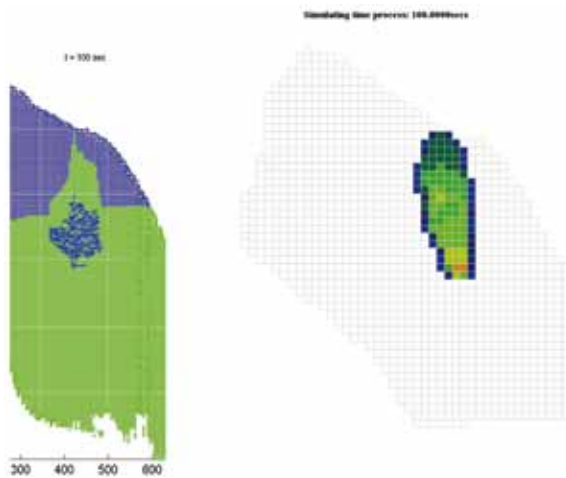


Fig. 22 - Comparison between Simul. N.9. and Flo-2D results for  $t=100$  secs

## REFERENCES

- BATCHELOR G.K. (1974) - *Introduction to fluid dynamics*. Cambridge University press, Cambridge.
- CRUDEN, D.M. (1991) - *A simple definition of a landslide*. Bulletin of the International Association of Engineering Geology, **43**: 27- 29.
- FLO-2D USER MANUAL (2009) - <http://www.flo-2d.com/downloads/flo-2d-2009-documentation/>
- GID REFERENCE MANUAL (2009) - <http://gid.cimne.upc.es/support/manuals>
- GINGOLD R.A., MONAGHAN J.J. (1977) - *Smoothed Particle Hydrodynamics: Theory and Application to Non-spherical Stars*. Monthly Notices of the Royal Astronomical Society, **181** (2): 375-389.
- IVERSON, R.M. (1997) - *The physics of debris flows*. Reviews of Geophysics, **35** (3): 245- 296.
- KOSHIZURA S., NOBE A., OKA Y. (1998). *Numerical analysis of breaking waves using the moving particle semi-implicit method*. Int. J. Numer. Methods Fluids, **26**: 751-769
- LIU G.R., LIU M.B. (2003) - *Smooth Particle Hydrodynamics*, A Meshfree Particle Method. World Scientific Printers, Singapore.
- LIU M.B., LIU G. R., ZONG Z., LAM K.Y. (2000) - *Numerical simulation of underwater explosion by SPH*. Advances in Computational Engineering & Science, 1475-1480.
- LUCY L.B. (1977) - *A numerical approach to the testing of the fission hypothesis*. Astron. Journal, **82**: 1013-1020.
- MONAGHAN J.J. (1994) - *Simulating free surface flows with SPH*. Journal of Computational Physics, **110**: 399-406.
- MONAGHAN J.J. & KOCHARYAN A. (1995) - *SPH simulation of multi-phase flow*. Computer Physics Computation, **87**: 225-235.
- MONAGHAN J.J. & LATTANZIO J.C. (1985). *A refined particle method for astrophysical problems*. Astronomy and astrophysics, **149**: 135-143.
- MORRIS J.P., ZHU Y., & FOX P. J. (1999) - *Parallel simulation of pore-scale flow through porous media*. Computers and Geotechnics, **25**: 227-246.
- RANDLES P.W. & LIBERSKY L.D. (1996) - *Smoothed Particle Hydrodynamics some recent improvements and applications*. Computer Methods in Applied Mechanics and Engineering, **138**: 375-408.
- REDDY J.N. (1993) - *An Introduction to the Finite Element Methods*. McGraw-Hill Book Co., New York.
- RÜBENKÖNIG O. (2006) - *The Finite Difference Method (FDM) - An introduction*. Albert Ludwigs University of Freiburg, Freiburg
- SWEGLE J.W. & ATTAWAY S.W. (1995) - *On the feasibility of using SPH for underwater explosion calculations*. Comput. Mechanics, **17**: 151-168.
- VICCIONE G. & BOVOLIN V. (2010) - *Simulating flash floods with SPH*. In: International workshop on EU Flood directive implementation in Mediterranean zone: Tools and challenges for efficient risk management. Barcellona. 17<sup>th</sup> June, 2010. (SPAIN).
- VICCIONE G., BOVOLIN V., PUGLIESE & CARRATELLI E. (2008) - *Defining and optimising algorithms for neighbouring particle identification in SPH fluid simulations*. International Journal for Numerical Methods in Fluids, **58** (6): 625-638.
- ZHU Y., FOX P.J. & MORRIS J.P. (1999) - *A pore-scale numerical model for flow through porous media*. International Journal for Numerical and Analytical methods in Geomechanics, **23**: 881-904.
- ZUKAS J.A. (1990). *High velocity impact*, John Wiley & Sons, New York.